

# Reconciliation of Weakly Correlated Information Sources Utilizing Generalized EXIT Chart

Hossein Mani, Tobias Gehring, Christoph Pacher, and Ulrik Lund Andersen

## Abstract

The current bottleneck of continuous-variable quantum key distribution (CV-QKD) is the computational complexity and performance of key reconciliation algorithms. CV-QKD requires capacity approaching error correcting codes in the low signal-to-noise (SNR) regime ( $\text{SNR} \ll 0$  dB) with very low code rates. Multilevel coding (MLC) combined with multistage decoding (MSD) can solve this challenge. Multi-edge-type low-density parity-check (MET-LDPC) codes are ideal for low code rates in the low SNR regime due to degree-one variable nodes. Here, we introduce the concept of generalized extrinsic information transfer (G-EXIT) charts for MET-LDPC codes and demonstrate how this tool can be used to analyze their convergence behavior. We calculate the capacity for each level in the MLC-MSD scheme and use G-EXIT charts to exemplarily find the best codes for some given thresholds. In comparison to the traditional density evolution method, G-EXIT charts offer a simple and fast asymptotic analysis tool for MET-LDPC codes.

## I. INTRODUCTION

The security of today's asymmetric cryptography and public key exchange systems like Rivest-Shamir-Adleman and Diffie-Hellman are based on mathematical complexity assumptions of basic problems like the discrete log problem and factorization of large primes [1]. The advent of the quantum computer or even an unexpected algorithmic innovation will immediately compromise their security with drastic consequences on the internet [2], [3].

One possible solution is quantum key distribution (QKD) which provides information theoretical secure cryptographic key exchange based on the properties of quantum mechanics. However both communication distance as well as the key generation rate is severely limited by the performance of information reconciliation which is an important part in every QKD protocol to ensure that both parties generate the same cryptographic key. This is in particular true for continuous variable (CV) QKD which is based on the modulation of coherent states and measurements of the amplitude and phase quadratures of the electromagnetic light field. To achieve high transmission distances reverse reconciliation has to be applied, i.e. Alice has to reconcile on Bob's measurement results. The main challenge here is the design of capacity approaching error correction codes for very low signal-to-noise ratios (SNR). For instance in [4] an SNR of  $-15.37$  dB was reported for a transmission distance of 80 km and in [5] an SNR of  $-16.198$  dB for 100 km.

Low density parity check codes (LDPC) in the multi-edge type (MET) variant [6] can be used in combination with multilevel coding - multistage decoding (MLC-MSD) to perform capacity approaching error correction for QKD with low SNR [7]. In the aforementioned paper about QKD over 80 km the authors developed a new code with rate 0.02 with an efficiency of 96.9%. This code was used in other works [8], however, the code has considerable complexity in its degree distribution (DD). The design of the codes with low complexity is desirable in terms of implementation complexity for encoder and decoder blocks. Designing an efficient capacity achieving DD with low complexity has been investigated in many works and different analytical as well as numerical techniques have been introduced [9]–[11].

C. Pacher is with the Center for Digital Safety & Security, AIT Austrian Institute of Technology GmbH, Giefinggasse 4, 1210 Vienna, Austria email: christoph.pacher@ait.ac.at

H. Mani, T. Gehring and U. L. Andersen are from Department of Physics, Technical University of Denmark, 2800 Kongens Lyngby, Denmark email: {hosma, tobias.gehring, ulrik.andersen}@fysik.dtu.dk.

Traditionally, code design for LDPC code is a time consuming process using a density evolution algorithm. In each iteration of the density evolution a vector of real values representing the density has to be updated which is computationally expensive. Due to this complexity many approximation methods for density evolution have been developed, for instance Gaussian approximation and Extrinsic Information Transfer (EXIT) charts [11], [12]. Nowadays, for a variety of binary memory-less channels, these asymptotic analysis tools are used for the optimization of the degree distribution. Specifically, for the binary erasure channel (BEC), design of capacity achieving codes can be carried out by matching the two curves of EXIT functions related to the variable node and check nodes degree distributions due to the area theorem [9]. In other binary input-output symmetric memory-less channels the Generalized area theorem and generalized EXIT (G-EXIT) charts can be used for the optimization problem [13].

Here, we introduce G-EXIT charts for MET-LDPC codes to provide a practical tool for their design and optimization. We use our tool to design new codes with rates 0.02, 0.05, and 0.1 with lower complexity. In general for a given input distribution we calculate the Shannon capacity for each level in the MLC-MSD scheme and present high efficiency MET-LDPC codes for various SNRs.

The organization of this paper is as follows. In Section II, we explain the system model for the reconciliation of the secret key rate and calculate the designed capacity rate for each level for a given input distribution. Section III, briefly reviews the basic concepts of the MET-LDPC codes and the extension of the density evolution for these codes. Then in Section IV, we introduce the concept of G-EXIT charts for MET-LDPC codes. Simulation results are presented in Section V, where we show how to use a G-EXIT chart for designing MET-LDPC codes. Finally, Section VI concludes the paper.

## II. SYSTEM MODEL

### A. Source Coding with side information and equivalent channel coding model

Information reconciliation is a method by which two parties that each possess a sequence of numbers agree on a *common* sequence of bits by exchanging one or more messages. Mathematically speaking, in CV-QKD the two sequences of numbers are joint instances of a bivariate random variable that follows a bivariate normal distribution. Physically, these sequences are obtained by one party generating coherent states in the quadrature phase space and the other party measuring them. In other words, in QKD two parties share correlated random variables and wish to agree on a common bit sequence. However, imperfect correlations introduced by the inherent shot noise of coherent states and noise in the quantum channel and the receiver, give rise to discrepancies in the two sequences of numbers which has to be corrected by exchanging additional information.

In reverse reconciliation, which is the focus of this paper, we assume that Alice reconciles her values to match Bob's. The reconciliation process can be fully described as a conventional information theory problem. This problem was first addressed by [14] as source coding with side information: Let Alice and Bob have access to two correlated information sources  $X_A$  and  $X_B$  which follow a joint probability distribution  $p_{X_A X_B}(x_A, x_B)$ . The two parties wish to distill a common binary string by exchanging information as shown in Fig. 1. In this configuration Bob sends to Alice a compressed version of his quantized symbols  $\{\mathcal{Q}(x_{B,i})\}_{i=1}^n$  and knows that Alice has access to the side information  $\{x_{A,i}\}_{i=1}^n$ . Based on the results presented in [14], [15], the conditional entropy  $H(\mathcal{Q}(X_B)|X_A)$  is (asymptotically) the minimum number of required bits for the reconciliation. Furthermore, it is more convenient to generate the syndromes using the codes with performance close to the Shannon capacity [15], [16]. In this case the parity check matrix of the error correction code can be used to generate the syndrome for the reconciliation problem. Thus an equivalent channel coding problem can be solved instead of the above mentioned source coding with side information. In the following we use an equivalent MLC-MSD scheme in order to design a lossless encoder decoder block.

### B. Slice Reconciliation based on MLC-MSD

Slice reconciliation using error correction codes can be described in two steps. The first step is called quantization and transforms the continuous Gaussian source  $X_B$  into an  $M$  bit source  $\mathcal{Q}(X_B)$ . There

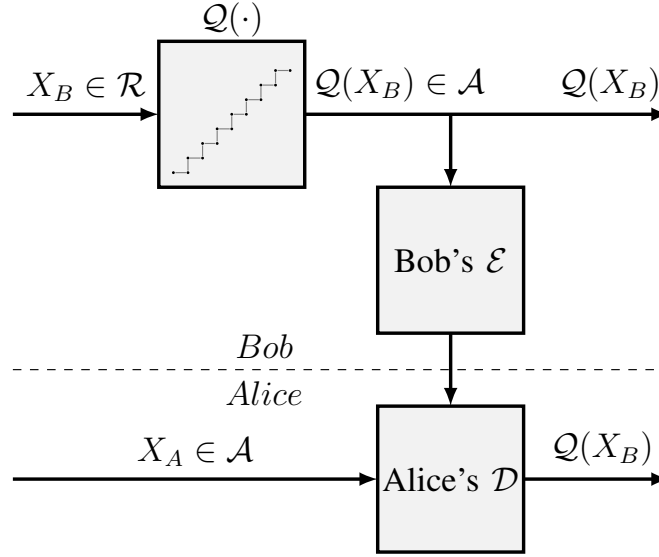


Fig. 1. Correlated source coding configuration. Correlated information sequences  $X_{B,0}, X_{B,1}, \dots$  and  $X_{A,0}, X_{A,1}, \dots$  are generated by a pair of discrete random variables  $X_A, X_B$  from a given bivariate distribution  $p_{X_A X_B}(x_A, x_B)$ . The encoder of each source is constrained to operate without knowledge of the other source, while the decoder has available both encoded binary message streams.

is an inherent information loss due to the discretization process of the source. The second step can be modeled with the channel coding scheme for MLC-MSD. In reverse reconciliation, Bob sends an encoding (compressed version) of  $Q(X_B)$  to Alice, such that she can infer  $Q(X_B)$  with high probability using her own source  $X_A$  as side information. In MLC-MSD each of these  $m$  levels are encoded independently at rate  $R_i^{ch}$  corresponding to the channel coding problem and the related compress rate for the source coding problem for each level would be  $R_i^s = 1 - R_i^{ch}$ . The block diagram for MLC-MSD scheme for the reverse reconciliation is depicted in Fig. 2.

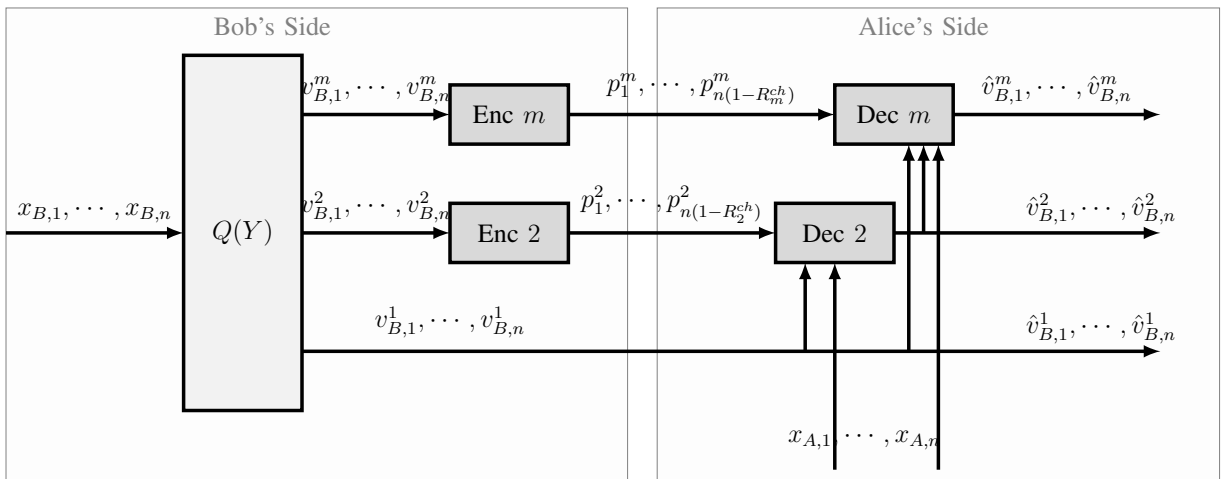


Fig. 2. The MLC-MSD scenario for the reverse reconciliation. First the input source is quantized into an  $m$ -bit source. Then each of the  $m$  sources is encoded and sent to Alice. The decoder has the side information from its own source and with the  $m$  encoded sources produces an estimate of the quantized source. Usually we transmit the least significant bits directly to the channel.

In the following we calculate the maximum capacity of the individual levels. Let's define the efficiency  $\beta$  as follows

$$\beta = \frac{H(Q(X_B)) - R^s}{I(X_B; X_A)}, \quad (1)$$

where  $I(X_B; X_A)$  is the mutual information and  $H(\mathcal{Q}(X_B)) - R^s$  is the net shared information between two parties [17] where,  $H(\cdot)$  is the entropy function and

$$R^s = \sum_{i=1}^m R_i^s = m - \sum_{i=1}^m R_i^{ch}.$$

Let's consider the ideal situation where the codes are capacity achieving with individual rates  $R_i^{ch} = C_i$ . Thus we have

$$\beta_Q = \frac{H(\mathcal{Q}(X_B)) - m + \sum_{i=1}^m C_i}{I(X_B; X_A)}, \quad (2)$$

where  $1 - \beta_Q$  denotes the deficiency when only the quantization part is considered. It is noteworthy to mention that  $H(\mathcal{Q}(X_B)) \leq m$  and  $\sum_{i=1}^m C_i = I(X_B; X_A)$ .

In general we can write

$$\beta = \frac{H(\mathcal{Q}(X_B)) - m + \sum_{i=1}^m R_i^{ch}}{I(X_B; X_A)}, \quad (3)$$

where  $R_i^{ch}$  denotes the individual code rates. Thus the practical efficiency of the reconciliation depends to the ability to design very good quantizers and very efficient error correction codes at rates close to  $I(\mathcal{Q}(X_B); X_A)$ . This efficiency belongs to equivalent channel coding problem. On the other hands, in [14], a lower bound to the correction rate  $R^{src}$ , is given by  $R^{src} \geq H(\mathcal{Q}(X_B)|X_A)$ .

We will now apply the MLC-MSD approach to design capacity achieving codes. Consider a modulation scheme with  $M = 2^m$ ,  $m > 1$ , signal points in a  $D$ -dimensional signal space, where the signal points are taken from the signal set  $\mathbf{S} = \{a_0, a_1, \dots, a_{M-1}\}$  with  $\mathbf{S} \in \mathbb{R}^D$ . Each signal point has its equivalent binary form defined by a (bijective) mapping  $a = \mathcal{M}(\mathbf{x})$  of binary address vectors  $\mathbf{x} = (x^0, x^1, \dots, x^{m-1})$  to signal points  $a \in \mathbf{S}$ . Two well defined mappings are binary and Gray mapping. As an example for the amplitude-shift keying (ASK) modulation with  $M = 2^3$ , in one dimensional signal space ( $D = 1$ ), the signal points are taken from  $\mathbf{S} = \{-7, -5, -3, -1, +1, +3, +5, +7\}$ . Any subset of the signal set  $\mathbf{S}$  can be labeled by a unique path. At partitioning level  $i$ , each subset is labeled by a unique path  $x^0, x^1, \dots, x^{i-1}$  with the following elements:

$$\mathbf{S}(x^0, \dots, x^{i-1}) = \{a = \mathcal{M}(\mathbf{x}) | \mathbf{x} = (x^0, \dots, x^{i-1}, b^i, \dots, b^{m-1})\}, \quad (4)$$

where  $b^j \in \{0, 1\}$ ,  $j = i, \dots, m-1$ . For more details about set partitioning and mapping see [7]. For example for the 8-ASK modulation with binary partitioning we have:

$$\begin{aligned} \mathbf{S}(x^0 = 1) &= \{a = \mathcal{M}(\mathbf{x}) | \mathbf{x} \in \{100, 101, 110, 111\}\} = \{-5, +3, -1, +7\} \\ \mathbf{S}(x^0 x^1 = 01) &= \{a = \mathcal{M}(\mathbf{x}) | \mathbf{x} \in \{010, 011\}\} = \{-3, +5\} \\ \mathbf{S}(x^0 x^1 x^2 = 010) &= \{a = \mathcal{M}(\mathbf{x}) | \mathbf{x} = \{010\}\} = \{-3\} \end{aligned}$$

### C. Capacity of Multi Level Coding

The derivation of the capacity of the multilevel coding scheme is presented by Theorem 1 in [7]. Based on that, the capacity  $C$  of a  $2^m$ -ary digital modulation scheme is equal to the sum of the capacities  $C_i$  of the equivalent channels  $i$  of a multilevel coding scheme,

$$C = \sum_0^{m-1} C_i. \quad (5)$$

This capacity can be approached via multilevel encoding and multistage decoding if and only if the individual rates  $R_i^{ch}$  are chosen to be equal to the capacity of the equivalent channels, i.e.  $R_i^{ch} = C_i$ . As

presented in [7], for given and fixed *a-priori* probabilities of signal points the capacity  $C_i$  of the equivalent channel  $i$  is given by the respective mutual information  $I(X_A; V_B^i | V_B^0 \cdots V_B^{i-1})$ ,

$$\begin{aligned} C_i &= I(X_A; V_B^i | V_B^0 \cdots V_B^{i-1}) \\ &= \mathbb{E}_{x^0 \dots x^{i-1}} \{C(\mathbf{S}(v_B^0 \cdots v_B^{i-1}))\} \\ &\quad - \mathbb{E}_{v_B^0 \dots v_B^i} \{C(\mathbf{S}(v_B^0 \cdots v_B^i))\} , \end{aligned} \quad (6)$$

where  $C(\mathbf{S}(v_B^0 \cdots v_B^i))$  denotes the capacity when using (only) the (sub)set  $\mathbf{S}(v_B^0 \cdots v_B^i)$  for a given and fixed *a-priori* probabilities  $\Pr\{a_k\} / \Pr\{\mathbf{S}(v_B^0 \cdots v_B^i)\}$ . For instance, according to (6) for 8-ASK we have

$$\begin{aligned} C^0 &= I(X_A; V_B^0) = C(\mathbf{S}) - \mathbb{E}_{v_B^0} \{C(\mathbf{S}(x^0))\} \\ C^1 &= I(X_A; V_B^1 | V_B^0) = \mathbb{E}_{v_B^0} \{C(\mathbf{S}(v_B^0))\} \\ &\quad - \mathbb{E}_{v_B^0 v_B^1} \{C(\mathbf{S}(v_B^0 v_B^1))\} \\ C^2 &= I(X_A; V_B^2 | V_B^0 V_B^1) = \mathbb{E}_{v_B^0 v_B^1} \{C(\mathbf{S}(v_B^0 v_B^1))\} \\ &\quad - \mathbb{E}_{v_B^0 v_B^1 v_B^2} \{C(\mathbf{S}(v_B^0 v_B^1 v_B^2))\} . \end{aligned}$$

Using (6), the problem of finding the individual capacities simplified to finding the capacity of the additive white Gaussian noise (AWGN) channel with discrete input variables  $a_k$ . In general, for a set of discrete input variables  $a_k$  from the input set  $\mathbf{S} = \{a_0, a_1, \dots, a_{M-1}\}$  and continuous output variable  $y = a_k + n$  where  $n$  has a Gaussian distribution with mean zero and variance  $\sigma^2$ , the average mutual information between  $\mathbf{S}$  and  $Y$  is given by

$$\begin{aligned} I(\mathbf{S}; Y) &= H(Y) - H(Y|\mathbf{S}) = \int_y f_Y(y) \log \frac{1}{f_Y(y)} dy \\ &\quad - \sum_{a_k \in \mathbf{S}} \int_y \Pr\{a_k\} f(y|a_k) \log \frac{1}{f(y|a_k)} dy \\ &= \int_y \sum_{a_k \in \mathbf{S}} \Pr\{a_k\} f_Y(y|a_k) \log \frac{1}{f_Y(y)} dy \\ &\quad - \sum_{a_k \in \mathbf{S}_{-\infty}} \int_{-\infty}^{\infty} \Pr\{a_k\} f(y|a_k) \log \frac{1}{f(y|a_k)} dy \\ &= \sum_{k=0}^{M-1} \int_{-\infty}^{\infty} \Pr\{a_k\} f_Y(y|a_k) \log_2 \frac{f_Y(y|a_k)}{f_Y(y)} dy , \end{aligned} \quad (7)$$

where in (7),  $\Pr\{a_k\}$  for  $0 \leq k \leq M-1$  denotes the discrete input probabilities and  $f_Y(y|a_k)$  denotes the conditional channel *probability density function* (PDF). The unconditional PDF for outcome  $y$  is given by

$$f_Y(y) = \sum_{k=0}^{M-1} \Pr\{a_k\} f_Y(y|a_k) . \quad (8)$$

When working with Gaussian distribution (7) can be simplified even more by replacing

$$f_Y(y|a_k) = \frac{1}{\sqrt{2\pi\sigma^2}} e^{-\frac{(y-a_k)^2}{2\sigma^2}} , \quad (9)$$

thus we have

$$\begin{aligned}
 I(\mathbf{S}; Y) &= \sum_{k=0}^{M-1} \int_{-\infty}^{\infty} \frac{\Pr\{a_k\}}{\sqrt{2\pi\sigma^2}} e^{-\frac{(y-a_k)^2}{2\sigma^2}} \log_2 \frac{e^{-\frac{(y-a_k)^2}{2\sigma^2}}}{f_Y(y)} dy, \\
 &= \sum_{k=0}^{M-1} \frac{\Pr\{a_k\}}{\sqrt{2\pi\sigma^2}} \\
 &\quad \left[ \int_{-\infty}^{\infty} e^{-\frac{(y-a_k)^2}{2\sigma^2}} \left( \frac{-(y-a_k)^2}{2\sigma^2} \log_2 e - \log_2 f_Y(y) \right) dy \right],
 \end{aligned}$$

which is the closed form formula for the individual levels in an AWGN channel with discretized input.

#### D. Individual and correlated rates

For uniform input distributions all the  $\Pr\{a_k\}$  are equal, while for the (discrete) Gaussian distributed inputs

$$\Pr\{a_k\} = K(\lambda) e^{-\lambda|a_k|^2}, \quad (10)$$

where

$$K(\lambda) = \left( \sum_{k=1}^M e^{-\lambda|a_k|^2} \right)^{-1} \quad (11)$$

normalizes the distribution. The parameter  $\lambda$  governs the trade off between average power of signal points  $\sigma_a^2$  and entropy  $H(\mathbf{S})$ . For  $\lambda = 0$ , we have a uniform distribution, whereas for  $\lambda \rightarrow \infty$ , only the two signal points closest to the origin remain ( $M$  even).

As an example, we demonstrate the simulation results for slice capacities for 64-ASK modulation, when the channel input as presented in Figure 3 is set to be (discrete) Gaussian distributed with  $\lambda = 0.0015$  which fixes the entropy  $H(\mathbf{S}) = 5.2325$ . In Figure 4 the individual capacities for the input distribution

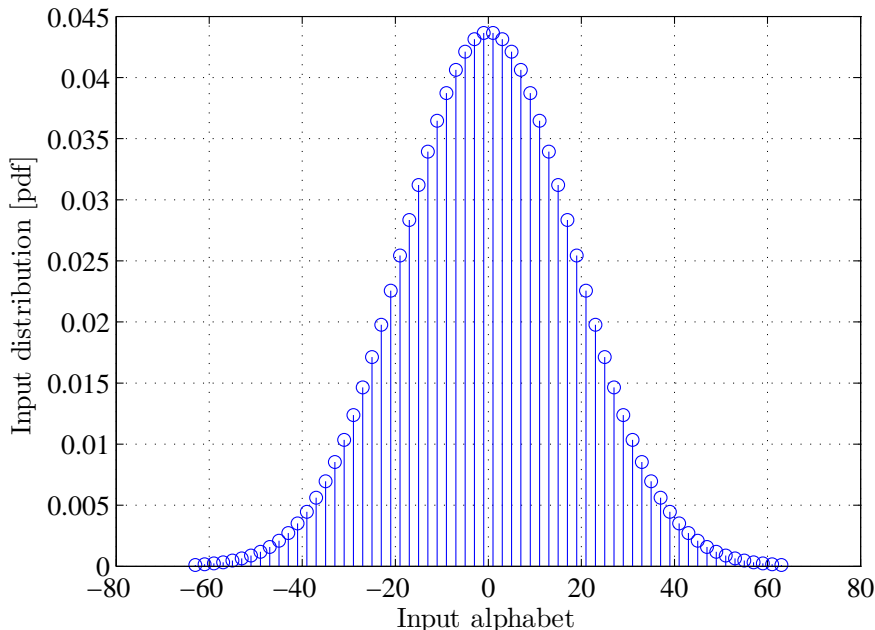


Fig. 3. The discrete Gaussian input distribution with parameter  $\lambda = 0.0015$ . For 64-ASK modulation with six levels.

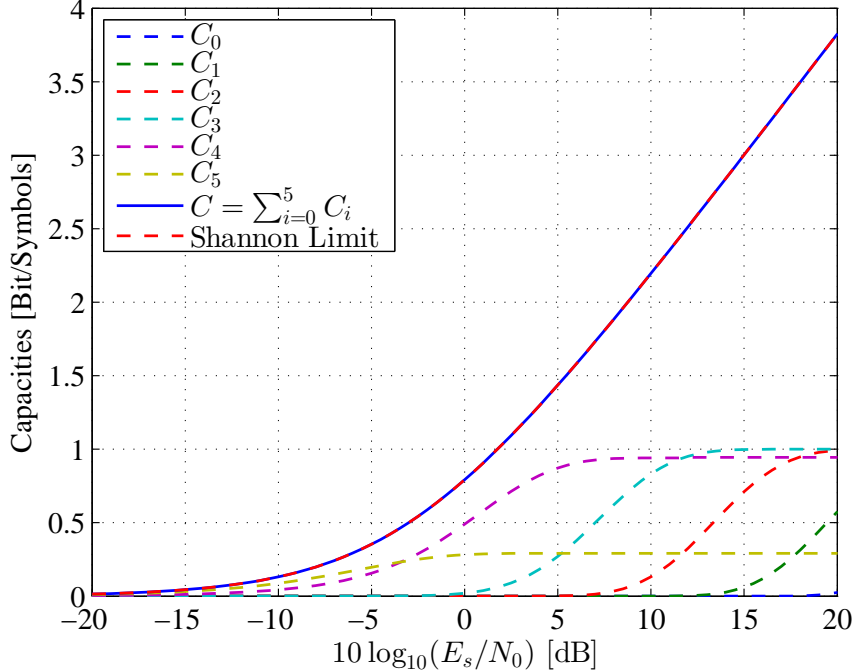


Fig. 4. The individual capacities for the 64-ASK modulation with binary partitioning versus  $E_s/N_0$ . In order to get a unified representation, x-axis is labeled by,  $E_s/N_0$  which is half of the signal-to-noise ratio, where  $E_s$  is the energy per symbol and  $N_0$  is the energy of the noise.

above are shown versus the SNR and the summation of the capacities is compared with the Shannon capacity of the AWGN channel.

In the MLC-MSD scheme, each level use different encoder and transmit its compressed data separately. We can assume that the individual levels are equi-probable binary sources but there exists some correlation between the levels. For example, in Figure 5, a 4-level quantizer is depicted for an input with Gaussian distribution also the equivalent binary outputs are presented under the curve, where rows represent the output of the levels and columns represent the binary mapping. As depicted, each row can be considered as an equi-probable binary source with elements zero and one. To show the correlation between the levels, assume that, the three least significant bits are known and are equal to “010” (denoted by red color), then the probability of being one for the most significant bit is not equal to being zero as denoted in Figure 5.

If we consider the correlation between the levels based on the input discrete Gaussian distribution then the individual rates for each level can be reformulated as follows:

$$R_i^* = C_i + \Delta_i, \quad (12)$$

where  $\Delta_i = 1 - H(V_B^i | V_B^0, \dots, V_B^{i-1})$ . From (6) and (12) it is clear that the  $1 - R_i^*$  is equal to the source coding rate given by Slepian-Wolf theorem [14]. Also using the chain rule for entropy a recursive calculation can be used to find the value of the conditional entropy as follows

$$\begin{aligned} H(V_B^0, \dots, V_B^i) &= H(V_B^0, \dots, V_B^{i-1}) \\ &\quad + H(V_B^i | V_B^0, \dots, V_B^{i-1}). \end{aligned}$$

For the same discrete Gaussian distribution, presented above we calculated the rates by considering the correlation between the individual sub-levels. The results are presented in Figure 6.

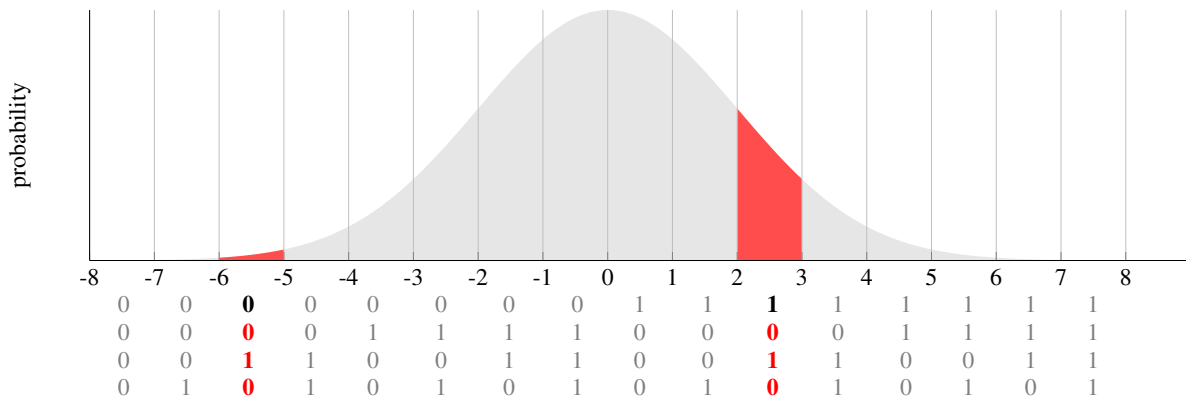


Fig. 5. (Color line) The binary outputs of a 4-level quantizer. The top row denotes the most significant bits and the lowest row represents the least significant bit. Individually each row can be considered as a source with equi-probable binary outputs. But knowing the correct values of low significant bits give information about the most significant bit.

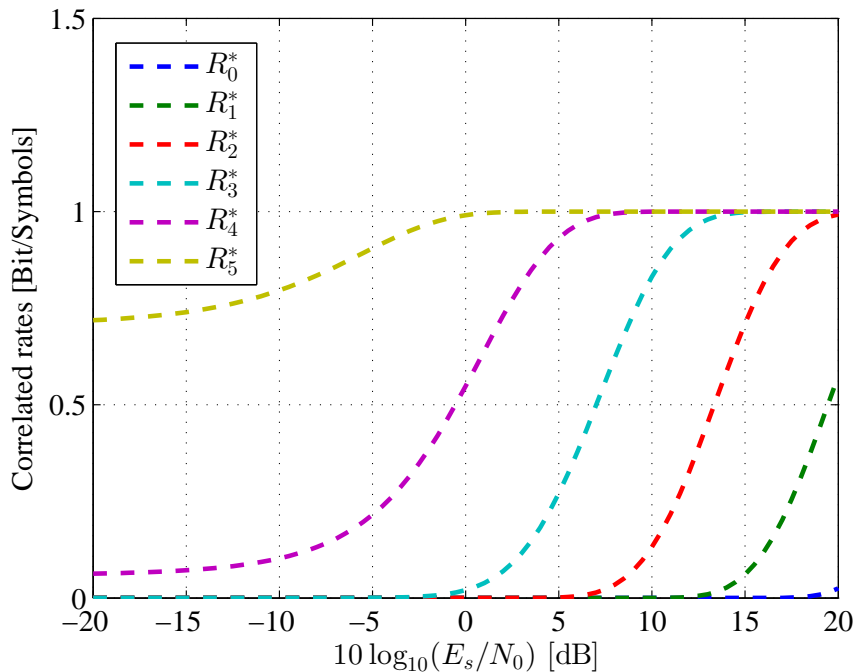


Fig. 6. (Color line) The correlated rates for the 64-ASK modulation with binary partitioning versus  $E_s/N_0$ .

### III. MET-LDPC CODES

#### A. MET-LDPC code ensemble

The Multi-edge-type LDPC (MET-LDPC) codes are a generalization of the concept of irregular LDPC codes. These codes provide improvements in performance and complexity by giving more flexibility over different edge types. In this structure each node is characterized by the number of connections (sockets) to edges of each edge-type. It is noteworthy to mention that an irregular LDPC code is a single-edge-type LDPC (SET-LDPC) code. Using MET-LDPC codes we are able to design capacity achieving codes without using very high-degree variable nodes which provides a less complex implementation. Also it exploits the advantage of using degree one variable nodes, which are very useful for designing LDPC codes at low rate and low SNR [6]. It is important to recall that in the case of SET-LDPC code the minimum variable node degree is 2.



A graph ensemble is specified through two multi-variable-polynomials, one associated to variable nodes and the other associated to check nodes. We denote these multi-variable-polynomials by

$$\nu(\mathbf{r}, \mathbf{x}) = \sum \nu_{\mathbf{bd}} \mathbf{r}^{\mathbf{b}} \mathbf{x}^{\mathbf{d}}, \quad \mu(\mathbf{x}) = \sum \mu_{\mathbf{d}} \mathbf{x}^{\mathbf{d}} \quad (13)$$

respectively, where in (13) we define the vectors  $\mathbf{b}, \mathbf{d}, \mathbf{r}, \mathbf{x}$  and the coefficients  $\nu_{\mathbf{bd}}$  and  $\mu_{\mathbf{d}}$  as follows. Let  $n_e$  denote the number of edge types and  $n_r$  denote the number of different channels over which the code-word bits can be transmitted. To represent the structure of the graph we introduce the following *node-perspective* multi-variable-polynomial representation. We interpret degrees as exponents. Let  $\mathbf{d} := (d_1, \dots, d_{n_e})$  be a multi-edge degree and let  $\mathbf{x} := (x_1, \dots, x_{n_e})$  denote (vector) variables. We write  $\mathbf{x}^{\mathbf{d}}$  for  $\prod_{i=1}^{n_e} x_i^{d_i}$ . Similarly, let  $\mathbf{b} := (b_0, \dots, b_{n_r})$  be a received degree and let  $\mathbf{r} := (r_0, \dots, r_{n_r})$  denote variables corresponding to received distributions. By  $\mathbf{r}^{\mathbf{b}}$  we mean  $\prod_{i=1}^{n_r} r_i^{b_i}$ . Typically, vectors  $\mathbf{b}$  will have one entry set to 1 and the rest set to 0. Finally, the coefficients  $\nu_{\mathbf{bd}}$  and  $\mu_{\mathbf{d}}$ , are non-negative reals corresponding to the fraction of variable nodes of type  $(\mathbf{bd})$  and the fraction of constraint nodes of type  $\mathbf{d}$  in the graph.

For example, let  $N$  be the length of the code-word, then for each constraint node degree type  $\mathbf{d}$  the quantity  $\mu_{\mathbf{d}}N$  is the number of constraint nodes of type  $\mathbf{d}$  in the graph. Similarly, the quantity  $\nu_{\mathbf{bd}}N$  is the number of variable nodes of type  $(\mathbf{bd})$  in the graph. We store these information in a table to introduce the structure of the graph. For instance a full description of a rate 0.02 MET-LDPC code ensemble with the following structure is presented in Table. I and Fig. 7.

$$\begin{aligned} \nu(\mathbf{r}, \mathbf{x}) &= 0.0498 r_2 x_1^2 x_2^2 + 0.0498 r_2 x_1^3 x_2^{45} + 0.9003 r_2 x_3 \\ \mu(\mathbf{x}) &= 0.0348 x_1^2 + 0.0449 x_1^4 + 0.7212 x_2^3 x_3^1 + 0.1791 x_2^1 x_3^1 \end{aligned}$$

TABLE I

TABLE PRESENTATION OF RATE 0.02 DEGREE STRUCTURE FOR A MET-LDPC CODE WITH 3 EDGE TYPES.

$\nu_{\mathbf{bd}}$	$\mathbf{b}$	$\mathbf{d}$	$\mu_{\mathbf{d}}$	$\mathbf{d}$
0.0498442		2 2 0	0.0347664	2 0 0
0.0498442	[0 1]	3 45 0	0.0449221	4 0 0
0.900312		0 0 1	0.721184	0 3 1
			0.179128	0 1 1

The edge perspective degree distribution can be described as a vector of multi-variable polynomials, for variable nodes and check nodes, respectively,

$$\begin{aligned} \lambda(\mathbf{r}, \mathbf{x}) &= \left( \frac{\nu_{x_1}(\mathbf{r}, \mathbf{x})}{\nu_{x_1}(\mathbb{1}, \mathbb{1})}, \frac{\nu_{x_2}(\mathbf{r}, \mathbf{x})}{\nu_{x_2}(\mathbb{1}, \mathbb{1})}, \dots, \frac{\nu_{x_{n_e}}(\mathbf{r}, \mathbf{x})}{\nu_{x_{n_e}}(\mathbb{1}, \mathbb{1})} \right) \\ \rho(\mathbf{x}) &= \left( \frac{\mu_{x_1}(\mathbf{x})}{\mu_{x_1}(\mathbb{1})}, \frac{\mu_{x_2}(\mathbf{x})}{\mu_{x_2}(\mathbb{1})}, \dots, \frac{\mu_{x_{n_e}}(\mathbf{x})}{\mu_{x_{n_e}}(\mathbb{1})} \right), \end{aligned} \quad (14)$$

where

$$\begin{aligned} \nu_{r_i}(\mathbf{r}, \mathbf{x}) &= \frac{\partial}{\partial r_i} \nu(\mathbf{r}, \mathbf{x}), \quad \nu_{x_i}(\mathbf{r}, \mathbf{x}) = \frac{\partial}{\partial x_i} \nu(\mathbf{r}, \mathbf{x}) \\ \mu_{x_i}(\mathbf{x}) &= \frac{\partial}{\partial x_i} \mu(\mathbf{x}) \end{aligned}$$

and  $\mathbb{1}$  denotes a vector of all 1s where the length being determined by context. The coefficients of  $\nu$  and  $\mu$  are constrained to ensure that the number of sockets of each type is the same on both sides (variable and check) of the graph. This gives rise to  $n_e$  linear conditions on the coefficients of  $\nu$  and  $\mu$  as follows

$$\nu_{x_i}(\mathbb{1}, \mathbb{1}) = \mu_{x_i}(\mathbb{1}), \quad i = 1, \dots, n_e.$$

Finally, the nominal code rate is given by

$$\text{rate} = \nu(\mathbb{1}, \mathbb{1}) - \mu(\mathbb{1}).$$

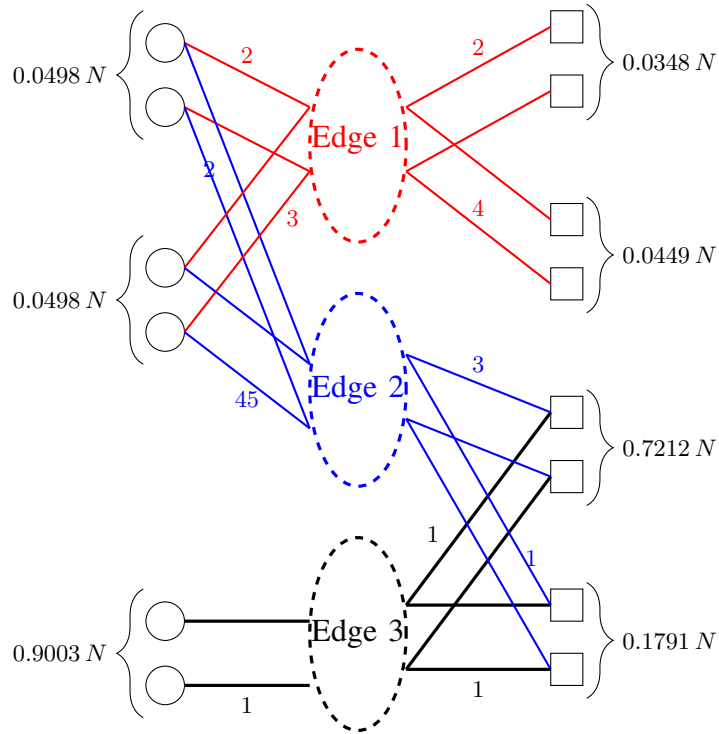


Fig. 7. Graphical representation of a three-edge type-LDPC code presented in Table I, where  $\circ$  represents the variable nodes and  $\square$  represents the check nodes. The number of nodes for different edge-types are shown as fractions of the code length  $N$ , where  $N$  is the number of transmitted code-word bits.

#### IV. GENERALIZED EXTRINSIC INFORMATION TRANSFER CHART

##### A. Belief Propagation and asymptotic analysis tools

Density evolution (DE) is the main tool for analyzing the average asymptotic behavior of the belief propagation (BP) decoders for MET-LDPC code ensembles with infinite block length and infinite number of iterations. The DE analysis is in general simplified by the all-one code word assumption, the channel symmetry and by going to log-likelihood ratio (LLR) domain [18]–[20]. Let us denote by  $\mathbf{P} = (P_1, \dots, P_{n_e})$ , vectors of symmetric densities where  $P_i$  is the density of messages carried on edge type  $i$ . Also assume that  $\mathbf{P}^l(\mathbf{Q}^l)$  denote the vector of messages passed from variable nodes to check nodes in iteration  $l$  assuming that  $\mathbf{P}^0(\mathbf{Q}) = \mathbf{Q}$ . Similarly, let  $\mathbf{R}$  be the received distributions. Then the following recursion represents the density evolution for MET-LDPC codes:

$$\mathbf{P}^{l+1} = \lambda(\mathbf{R}, \rho(\mathbf{P}^l)), \quad (15)$$

where,  $\rho(\mathbf{x})$  and  $\lambda(\mathbf{r}, \mathbf{x})$  are presented in (14). Detailed calculation of the density evolution for MET-LDPC codes can be found in Section II-B of [18].

##### B. Generalized-EXIT function, G-EXIT curve and Dual G-EXIT curve

The original idea behind the G-EXIT chart method is to demonstrate the decoding process using a suitable one-dimensional representation of the densities [21]. The G-EXIT chart is visualized on the basis of two G-EXIT curves that represent the action of the different types of nodes. Considering the fact that for MET-LDPC codes, the DE tracks  $n_e$  message densities as presented in (14) and (15), the G-EXIT chart for MET-LDPC codes is also expanded to a vector of  $n_e$  components. This makes the G-EXIT analysis tools unpractical when the number of edges are more than three ( $n_e \geq 3$ ). Intuitively we present again a one-dimensional G-EXIT chart by exploiting appropriate convolution in variable nodes and constraint nodes before applying the G-EXIT projection to the densities.

Based on the results of [13], given two families of  $L$ -densities  $\{c_{\epsilon_i}\}$  and  $\{a_{\epsilon}\}$  parameterized by  $\epsilon$ , the G-EXIT function can be represented as follows:

$$G(c_{\epsilon_i}, a_{\epsilon}) = \frac{\int_z \int_w a_{\epsilon}(z) \frac{\partial c_{\epsilon_i}(\omega)}{\partial \epsilon} \cdot \log_2(1 + e^{-z-\omega}) d\omega dz}{\int_w \frac{\partial c_{\epsilon_i}(\omega)}{\partial \epsilon} \cdot \log_2(1 + e^{-\omega}) d\omega}, \quad (16)$$

and the G-EXIT kernel is defined as

$$l^{c_{\epsilon_i}}(z) = \frac{\int_w \frac{\partial c_{\epsilon_i}}{\partial \epsilon} \cdot \log_2(1 + e^{-z-\omega}) d\omega}{\int_w \frac{\partial c_{\epsilon_i}}{\partial \epsilon} \cdot \log_2(1 + e^{-\omega}) d\omega}. \quad (17)$$

Consequently, the G-EXIT curve is given in parametric form by  $\{H(c_{\epsilon_i}), G(c_{\epsilon_i}, a_{\epsilon})\}$ , where

$$H(c_{\epsilon_i}) = \int_{-\infty}^{\infty} c_{\epsilon_i}(\omega) \log(1 + e^{-\omega}) d\omega.$$

According to (15), the DE provides two vectors with  $n_e$ -components of densities for the variable nodes and check nodes, respectively. In order to plot the one-dimensional G-EXIT chart, these  $n_e$  densities corresponding to each edge type will be combined to a single family of densities based on (13). Thus for the MET-LDPC codes the combination of densities for variable nodes and check nodes with  $n_e$  edges are

$$c_{\epsilon_i} = \sum \nu_{\text{bd}} \mathbf{R}^{\text{b}} \otimes \mathbf{P}^{\text{d}}, \quad (18)$$

$$a_{\epsilon} = \sum \mu_{\text{d}} \mathbf{Q}^{\text{d}}, \quad (19)$$

where  $\mathbf{P}^{\text{d}}$  denotes  $\bigotimes_{j=1}^{n_e} P_i^{\otimes d_i}$ , similarly  $\mathbf{R}^{\text{b}}$  denotes  $\bigotimes_{j=1}^{n_e} R_i^{\otimes b_i}$ , and  $\otimes$  denotes convolution in variable nodes. In a similar way  $\mathbf{Q}^{\text{d}}$  denotes  $\boxtimes_{j=1}^{n_e} Q_i^{\boxtimes d_i}$ , and  $\boxtimes$  denote the convolution of check nodes.

According to [13] the dual G-EXIT curve is defined in parametric form as  $\{G(a_{\epsilon}, c_{\epsilon_i}), H(a_{\epsilon})\}$ , where

$$G(a_{\epsilon}, c_{\epsilon_i}) = \frac{\int_z \int_w c_{\epsilon_i}(\omega) \frac{\partial a_{\epsilon}(z)}{\partial \epsilon} \cdot \log_2(1 + e^{-z-\omega}) d\omega dz}{\int_z \frac{\partial a_{\epsilon}(z)}{\partial \epsilon} \cdot \log_2(1 + e^{-z}) dz}, \quad (20)$$

and

$$H(a_{\epsilon}) = \int_{-\infty}^{\infty} a_{\epsilon}(z) \log(1 + e^{-z}) dz. \quad (21)$$

It is proven that for a binary linear code and transmission over *Binary Memoryless Symmetric* (BMS) channel that the G-EXIT and dual G-EXIT curves have an area equal to  $r(C)$ , the rate of the code [13].

## V. IMPLICATION OF THE G-EXIT CHART IN THE CODE DESIGN

### A. Examples of G-EXIT charts for MET-LDPC codes

In this section we present some examples of MET-LDPC codes and try to find the threshold of the codes using the G-EXIT chart method. We start with the rate 0.02 MET-LDPC code in Table. I. The Shannon limit for rate 0.02 is equal to SNR = -15.5108 dB ( $\sigma_{Sh}^* = 5.9640$ ) and our proposed code has the threshold equal to -15.2394 dB ( $\sigma_{DE}^* = 5.7806$ ) which is just 0.2714 dB away from capacity. With  $E_b$  being the energy per bit and  $N_0$  being the energy of the noise, the relation between  $E_b/N_0$ , the SNR and  $\sigma$  for an AWGN channel with binary transmission is

$$\frac{E_b}{N_0} [\text{dB}] = \text{SNR} [\text{dB}] - 10 \log_{10}(2 \cdot \text{rate}),$$

$$\sigma = \frac{1}{\sqrt{2 \cdot \text{rate} \cdot \frac{E_b}{N_0} [\text{linear}]}}.$$

Also, using (14) the density evolution vector of multi-variable polynomials can be written as

$$\lambda(\mathbf{r}, \mathbf{x}) = \left( 0.6r_2 x_1^2 x_2^{45} + 0.4r_2 x_1 x_2^2, 0.9574r_2 x_1^3 x_2^{44} + 0.0426 r_2 x_1^2 x_2, r_2 \right),$$

$$\rho(\mathbf{x}) = \left( 0.7210 x_1^3 + 0.2790 x_1^1, 0.9235 x_2^2 x_3 + 0.0765 x_3, 0.801 x_2^3 + 0.1990 x_2 \right),$$

where by replacing the vectors of variables of  $\mathbf{r}$  and  $\mathbf{x}$  with vectors of densities  $\mathbf{R}_{ch}$ ,  $\mathbf{P}_i$  and  $\mathbf{Q}_i$  for channel, check nodes and variable nodes respectively we have the MET-DE. Figure 8 shows the convergence behavior of each edge for the above mentioned code.

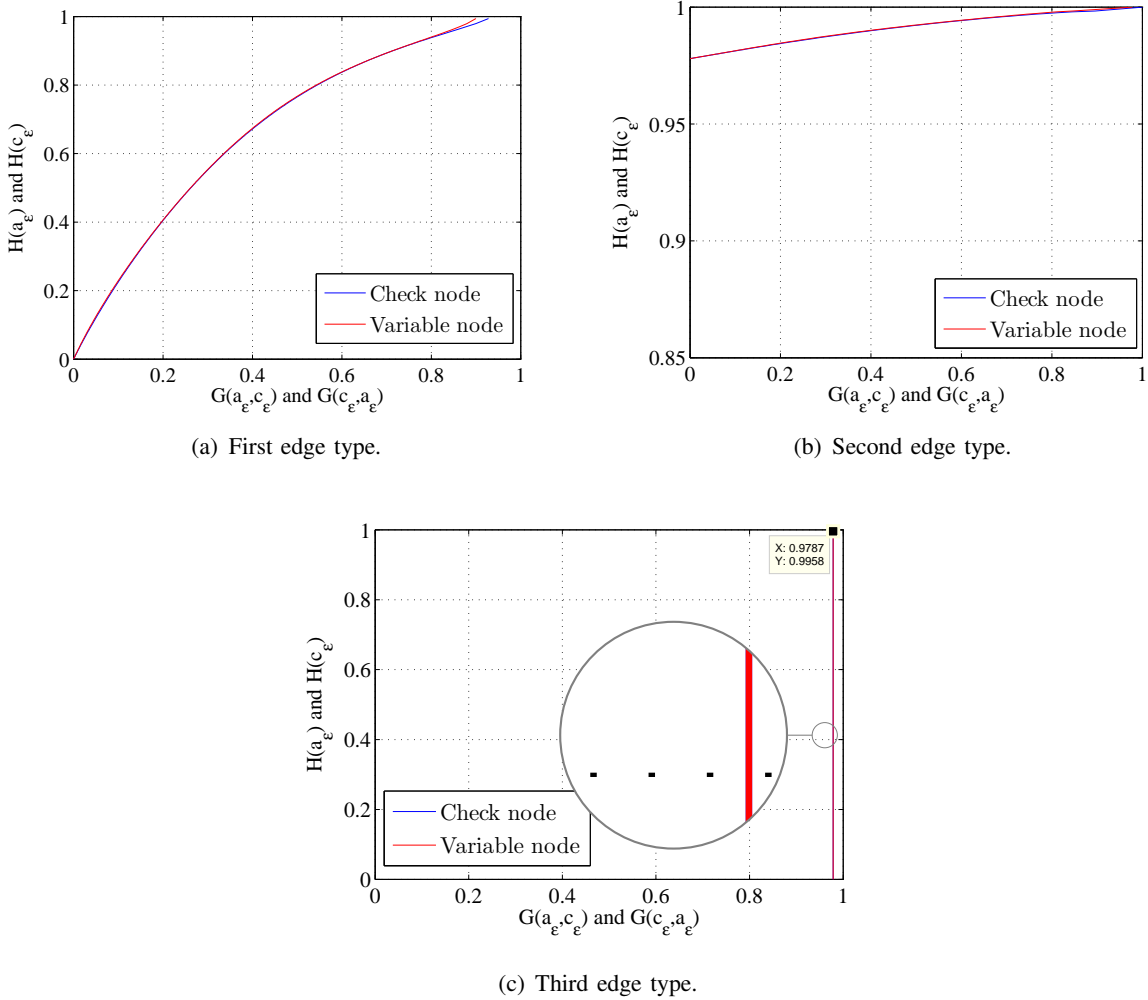


Fig. 8. The G-EXIT charts for separate edges for rate 0.02 MET-LDPC code. When the code converges at a specific threshold value we are able to plot the G-EXIT charts separately by applying the G-EXIT operators for densities at each edge.

It is noteworthy to mention that there is a single edge type variable node for this MET-LDPC code (c.f. Table I). This node applies a fixed channel density at each iteration of the DE. The corresponding G-EXIT curve for this edge is plotted in Fig. 8(c), which is constructed from two completely matching vertical lines at a specific  $x$ -value which denotes the entropy of the channel  $H(\sigma_{DE}^*) = 0.9787$ .

Finally, to see the convergence of a MET-LDPC code in a single plot, we used the overall combination of the edges with appropriate combination in check nodes and variable nodes according to (18)-(19). The results are presented in Figure 9.

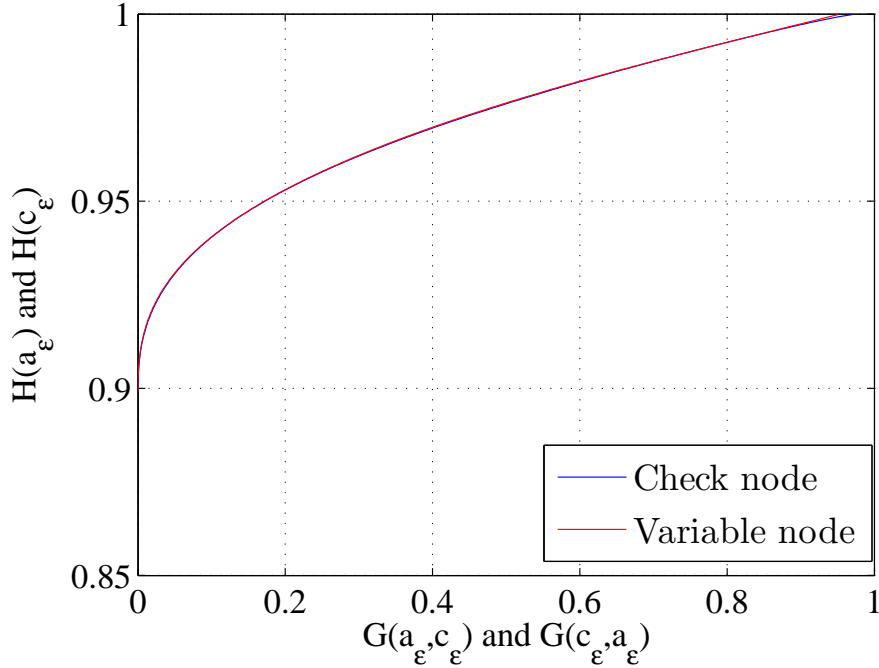


Fig. 9. The G-EXIT chart for rate the 0.02 MET-LDPC code. The SNR dB for this code is  $-15.23$  dB which is equivalent to  $\sigma_{DE}^* = 5.7806$ . The red line is for the variable node and the blue line stands for the check node.

As a second example, Figure 10 demonstrates the G-EXIT chart for a rate 0.1 MET-LDPC code. The node perspective degree structure of this code is presented in Table II and the polynomial form for this code is

$$\begin{aligned} \nu(\mathbf{r}, \mathbf{x}) &= 0.0607r_2x_1^2x_2^{21} + 0.0633r_2x_1^3x_2^{21} + 0.8760r_2x_3, \\ \mu(\mathbf{x}) &= 0.0239x_1^{13} + 0.8632x_2^3x_3^1 + 0.0128x_2^1x_3^1. \end{aligned}$$

TABLE II  
TABLE PRESENTATION OF THE DEGREE STRUCTURE FOR A RATE 0.1 MET-LDPC CODE

$\nu_{\mathbf{bd}}$	$\mathbf{b}$	$\mathbf{d}$	$\mu_{\mathbf{d}}$	$\mathbf{d}$
0.0606643	[0 1]	2 21 0	0.0239311	13 0 0
0.0632668		3 21 0	0.863242	0 3 1
0.8760690		0 0 1	0.0128269	0 1 1

The code has  $n_e = 3$  edge type and the threshold of this code in an AWGN channel using DE is equal to  $E_b/N_0 = -1.1751$  dB ( $\sigma_{DE}^* = 2.5600$ ). The Shannon limit is equal to  $-1.2872$  dB ( $\sigma_{Sh}^* = 2.5933$ ) and this code is just 0.1121 dB away from capacity. The corresponding G-EXIT curve for this code is plotted in Fig. 10.

As a third example, Table III shows the degree structure of a rate 0.05 MET-LDPC code. The threshold of this code is equal to  $E_b/N_0 = -1.2999$  dB ( $\sigma_{DE}^* = 3.6728$ ). The Shannon limit is equal to  $-1.4404$  dB ( $\sigma_{Sh}^* = 3.7327$ ) and this code is just 0.14 dB away from capacity. The G-EXIT chart for this code is plotted in Fig. 11.

As fourth example, Figure 12 shows the G-EXIT chart for a rate 0.5 MET-LDPC code presented in Table IV. This code was first published in [6] and has a threshold equal to  $E_b/N_0 = 0.305$  dB ( $\sigma_{DE}^* = 0.9655$ ).

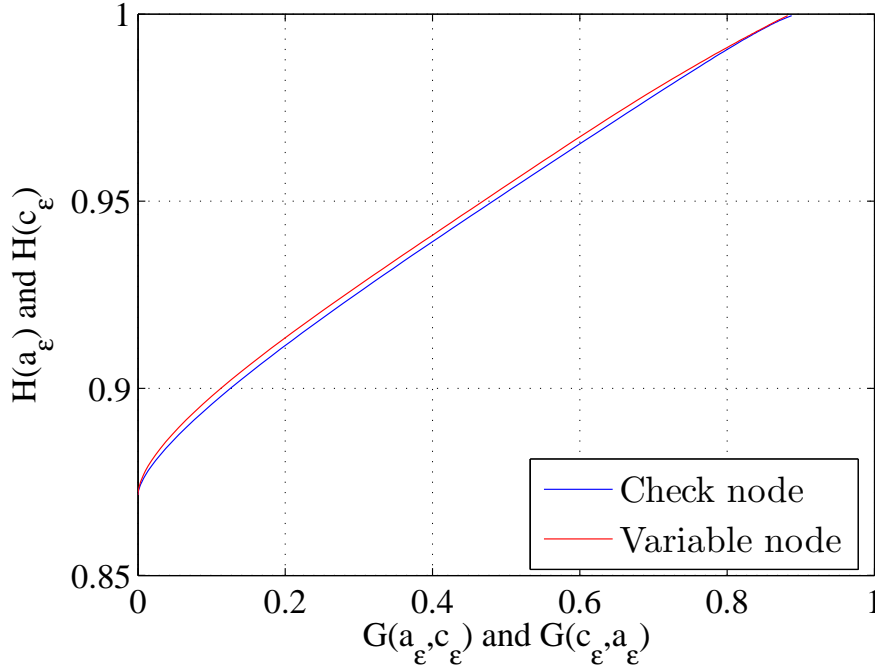


Fig. 10. The G-EXIT chart for rate 0.1 MET-LDPC code. The threshold of the code is  $E_b/N_0 = -1.1751$  dB. The corresponding curves are plotted at  $E_b/N_0 = -1.07$  dB.

TABLE III  
TABLE PRESENTATION OF THE DEGREE STRUCTURE FOR A RATE 0.05 MET-LDPC CODE

$\nu_{bd}$	<b>b</b>	<b>d</b>	$\mu_d$	<b>d</b>
0.05625	[0 1]	2 21 0	0.02656	3 0 0
0.04375		3 24 0	0.02344	7 0 0
0.90000		0 0 1	0.46875	0 2 1
			0.43125	0 3 1

TABLE IV  
TABLE PRESENTATION OF THE DEGREE STRUCTURE FOR A RATE 0.5 MET-LDPC CODE [6]

$\nu_{bd}$	<b>b</b>	<b>d</b>	$\mu_d$	<b>d</b>
0.2	1 0	0 3 3 0	0.1	3 2 0 0
0.5	0 1	2 0 0 0	0.4	4 1 0 0
0.3	0 1	3 0 0 0	0.2	0 0 3 1
0.2	0 1	0 0 0 1		

### B. Convergence behavior using the G-EXIT chart

Now we use the graphical presentation to demonstrate the convergence behavior of the code structure which we will exemplify for the rate 0.5 MET-LDPC code (c.f. IV). As depicted in Fig. 12, the two curves are matched to each other and the threshold of this code is 0.305 dB. In Fig. 13 the G-EXIT charts are plotted for this code for two different  $E_b/N_0 \in \{0.605, 0.005\}$ , which are  $E_b/N_0^{DE} \pm 0.3$ . It is possible to translate convergence behavior of the code by monitoring the status of the G-EXIT curves.

For  $E_b/N_0$  smaller than the threshold the code is not able to correct errors. In this case the two curves cross each other in the G-EXIT chart, see Fig. 13(a). For  $E_b/N_0 = 0.63$  dB, a value larger than the threshold, the corresponding G-EXIT chart is plotted in Fig. 13(b). The extra gap shows that the corresponding MET-LDPC code is still able to correct the errors even with a worse channel.

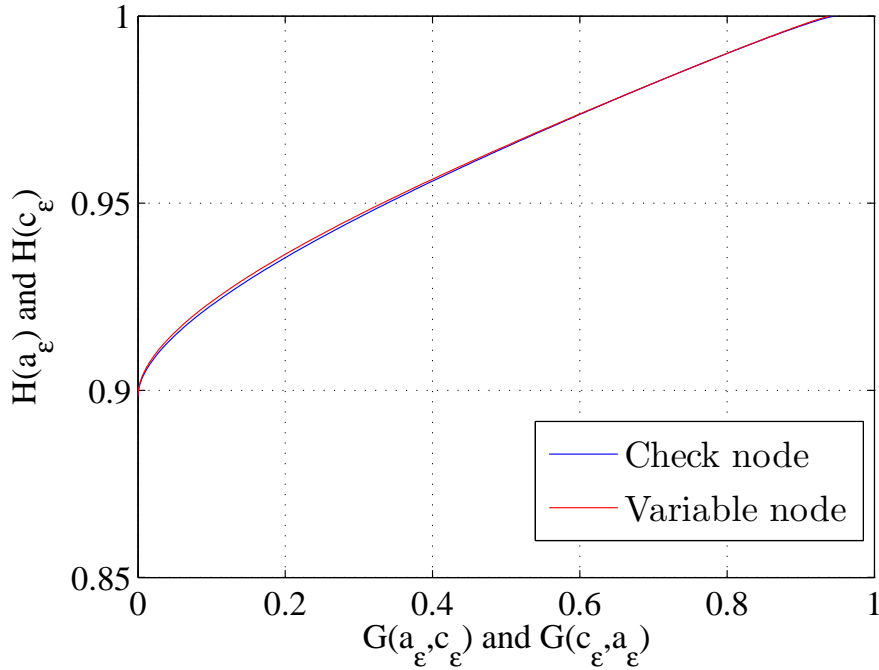


Fig. 11. The G-EXIT chart for rate 0.05 MET-LDPC code. The threshold of the code is  $E_b/N_0 = -1.299$  dB.

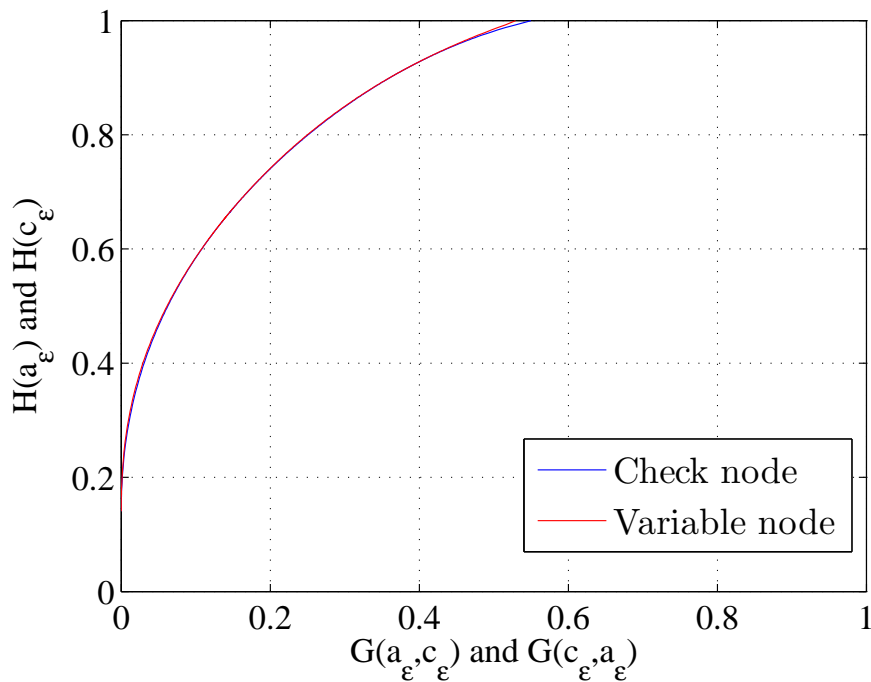


Fig. 12. The G-EXIT chart for rate 0.5 MET-LDPC code. The threshold of the code is  $E_b/N_0 = 0.305$  dB which is just 0.0700 dB away from Shannon limit.

### C. Gaussian assumption and complexity reduction

For SET LDPC codes for the BI-AWGN channel the well-known one dimensional Gaussian approximation can be used to determine the convergence threshold [12], [16], [22]–[26]. In case the check

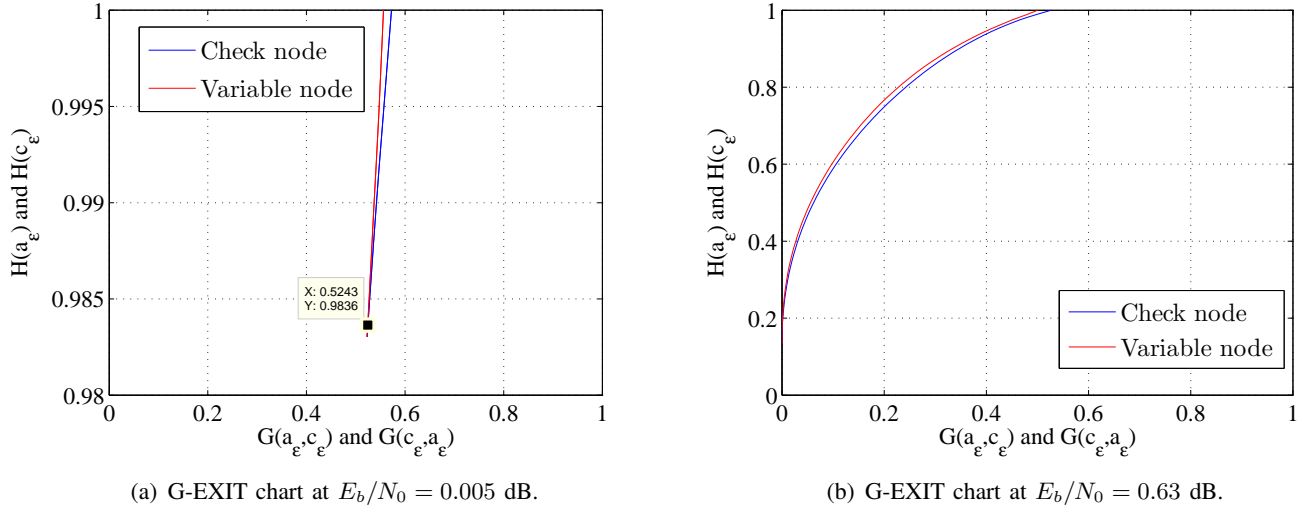


Fig. 13. The convergence behavior of the G-EXIT charts for rate 0.5 MET-LDPC code. Figures 13(a) and 13(b) show the convergence behavior of the code for a noise variance of  $\sigma = 0.9994$  and  $\sigma = 0.9327$ , respectively. For the former the code does not converge which can be seen by the crossing lines, while for the latter the code converges.

node degrees are small and the variable degrees are large enough, the PDF of both the variable and the check nodes can be approximated by a Gaussian distribution for all input and intermediate densities. The Gaussian PDF is thereby determined by its mean. It is thus enough to trace only a single parameter during the BP decoding algorithm.

For MET-LDPC this Gaussian approximation is not valid [18]. In this part we introduce a new analysis tool for MET-LDPC codes on AWGN channels which is significantly more accurate than the conventional Gaussian approximation. In our proposed method we assume a Gaussian distribution only for messages from variable nodes to check nodes. In comparison to other existing methods which assume Gaussian approximation for both check nodes and variable nodes [18], our method calculates the check node PDFs based on check node operations. To show the accuracy of this method we combined the G-EXIT operator to our approximation method and found the threshold and convergence behavior of the codes. Simulation results show that our proposed method provides an accurate estimate of the convergence behavior and the threshold of the code.

For better understanding we plotted the evolution of the intermediate densities in the DE algorithm for the rate 0.1 MET-LDPC code. As depicted in Fig. 14, the Gaussian approximation is not valid for the check node output densities, but at the variable node outputs, the intermediate densities can be described by symmetric Gaussian distributions. Then in the process of the G-EXIT chart we can gradually change the mean of the Gaussian distribution from 0 to  $\infty$ <sup>1</sup>, and calculate the G-EXIT curves for the variable nodes and check nodes using (18)-(20).

We also found the convergence threshold for the rate 0.1 MET-LDPC code presented in Table II using our new proposed method. In comparison with DE the algorithm will find the convergence threshold very fast and the estimated threshold is  $E_b/N_0 = -1.0517$  dB ( $\sigma_{App}^* = 2.5234$ ). The threshold of the code given by DE was  $-1.1751$  dB ( $\sigma_{DE}^* = 2.5600$ ). The convergence behavior of this code is plotted in Fig. 15 when the intermediate densities at the variable nodes are assumed to be symmetric Gaussian.

Finally, to show the accuracy of this method, Table V shows the convergence threshold for some MET-LDPC codes using our G-EXIT method when Gaussian approximation is used in the variable node output ( $\sigma_{App}^*$ ). The results are compared with the exact threshold given by density evolution  $\sigma_{DE}^*$ . In addition, we count the number of iterations for the DE to achieve the error probability equal to  $10^{-10}$ . It shows the

<sup>1</sup>By  $\infty$  we mean very large value for the LLR. We assume that in LLR domain  $+25$  can be considered a large value and in this case we have almost zero error probability.



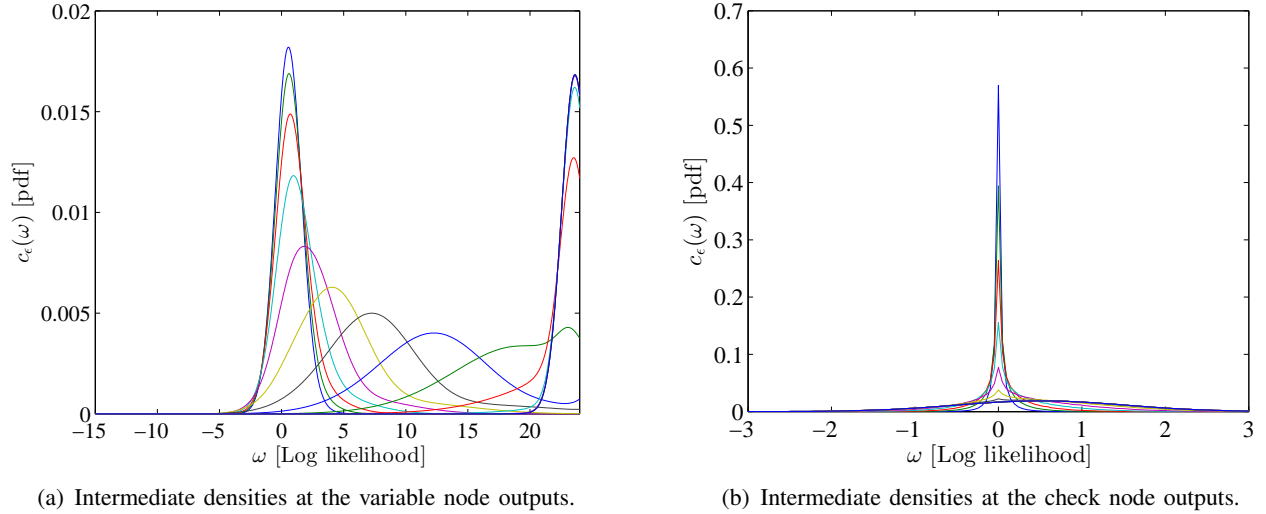


Fig. 14. The intermediate densities from iteration 1 to iteration 20, where the error probability is less than  $10^{-10}$  for rate 0.1 MET-LDPC code and  $E_b/N_0 = 0.6$  dB.

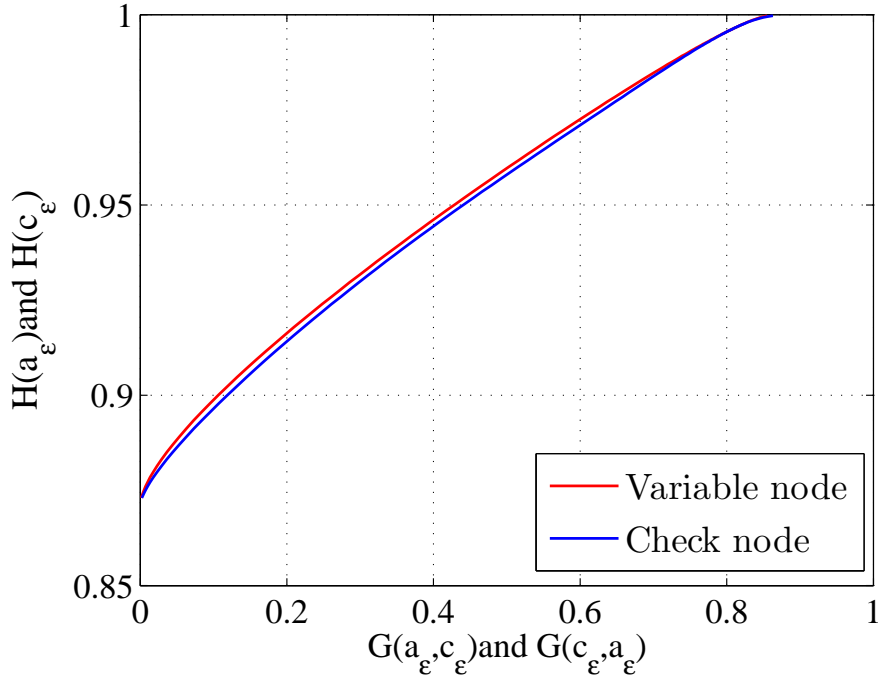


Fig. 15. The G-EXIT chart for the rate 0.1 MET-LDPC code when the intermediate densities at the variable nodes are assumed to be symmetric Gaussian. The threshold of the code given by the G-EXIT chart is  $-1.0517$  dB.

speed of these codes at specific SNRs.

## VI. CONCLUSION

In this paper we introduced the powerful tool and concept of the G-EXIT charts for MET-LDPC codes which can be used to design very efficient codes in a multi-level coding structure for very low rate and SNR which is required by certain applications like CV-QKD. Furthermore, we proposed a new approximation method for the density evolution. Our simulation results show that our approximation method provides

TABLE V  
COMPARISON OF THE CONVERGENCE THRESHOLD FOR DIFFERENT MET-LDPC CODES USING DENSITY EVOLUTION AND OUR PROPOSED APPROXIMATION METHOD. THE ERRO PROBABILITY IS SET TO BE  $10^{-10}$ .

rate	Structure	$\sigma_{DE}^*$	$\sigma_{APP}^*$	$\sigma_{Sh}^*$	Iterations	Efficiency
0.02	Section B, [8]	5.9016	5.7501	5.9640	502	97.94 %
0.02	Table I	5.7806	5.6425	5.9640	784	94.01 %
0.10	Table II	2.5600	2.5234	2.5933	382	97.62 %
0.05	Table III	3.6728	3.6308	3.7327	624	96.92 %
0.50	Table IV	0.9656	0.9627	1.00	1061	95.11 %

accurate approximation for the threshold of the MET-LDPC codes with accuracy equal to 98% and 99% for rates 0.02 and 0.5, respectively. With this approximation algorithm and the G-EXIT chart we can limit the calculations to SNRs close to the threshold which drastically reduces the run-time in comparison with the conventional density evolution algorithm. Using these tools we designed a new MET-LDPC code with rate 0.02 with reduced complexity in the code structure. Using 6 individual levels of MLC-MSD which is equivalent to a 64-ASK modulation, we designed a multi-level coding system close to the Shannon capacity at SNR =  $-15.4195$  dB.

## REFERENCES

- [1] P. W. Shor, "Polynomial-time algorithms for prime factorization and discrete logarithms on a quantum computer," *SIAM review*, vol. 41, no. 2, pp. 303–332, 1999.
- [2] D. Mayers, "Unconditional security in quantum cryptography," *J. ACM*, vol. 48, no. 3, pp. 351–406, May 2001. [Online]. Available: <http://doi.acm.org/10.1145/382780.382781>
- [3] H.-K. Lo and H. F. Chau, "Unconditional security of quantum key distribution over arbitrarily long distances," *Science*, vol. 283, no. 5410, pp. 2050–2056, 1999. [Online]. Available: <http://science.sciencemag.org/content/283/5410/2050>
- [4] P. Jouguet, S. Kunz-Jacques, and A. Leverrier, "Long-distance continuous-variable quantum key distribution with a gaussian modulation," *Physical Review A*, vol. 84, no. 6, p. 062317, 2011.
- [5] D. Huang, P. Huang, D. Lin, and G. Zeng, "Long-distance continuous-variable quantum key distribution by controlling excess noise," *Scientific reports*, vol. 6, p. 19201, 2016.
- [6] T. Richardson, R. Urbanke *et al.*, "Multi-edge type LDPC codes," in *Workshop honoring Prof. Bob McEliece on his 60th birthday, California Institute of Technology, Pasadena, California, 2002*, pp. 24–25.
- [7] U. Wachsmann, R. F. H. Fischer, and J. B. Huber, "Multilevel codes: theoretical concepts and practical design rules," *IEEE Transactions on Information Theory*, vol. 45, no. 5, pp. 1361–1391, Jul 1999.
- [8] M. Milicevic, C. Feng, L. M. Zhang, and P. G. Gulak, "Key reconciliation with low-density parity-check codes for long-distance quantum cryptography," *arXiv preprint arXiv:1702.07740*, 2017.
- [9] P. Oswald and A. Shokrollahi, "Capacity-achieving sequences for the erasure channel," *IEEE Transactions on Information Theory*, vol. 48, no. 12, pp. 3017–3028, Dec 2002.
- [10] H. D. Pfister, I. Sason, and R. Urbanke, "Capacity-achieving ensembles for the binary erasure channel with bounded complexity," *IEEE Transactions on Information Theory*, vol. 51, no. 7, pp. 2352–2379, July 2005.
- [11] H. Saeedi and A. H. Banihashemi, "New sequences of capacity achieving LDPC code ensembles over the binary erasure channel," *IEEE Transactions on Information Theory*, vol. 56, no. 12, pp. 6332–6346, Dec 2010.
- [12] M. Ardakani and F. R. Kschischang, "A more accurate one-dimensional analysis and design of irregular LDPC codes," *IEEE Transactions on Communications*, vol. 52, no. 12, pp. 2106–2114, Dec 2004.
- [13] C. Measson, A. Montanari, T. J. Richardson, and R. Urbanke, "The generalized area theorem and some of its consequences," *IEEE Transactions on Information Theory*, vol. 55, no. 11, pp. 4793–4821, Nov 2009.
- [14] D. Slepian and J. Wolf, "Noiseless coding of correlated information sources," *IEEE Transactions on Information Theory*, vol. 19, no. 4, pp. 471–480, July 1973.
- [15] M. Bloch, A. Thangaraj, S. W. McLaughlin, and J. M. Merolla, "LDPC-based Gaussian key reconciliation," in *2006 IEEE Information Theory Workshop - ITW '06 Punta del Este*, March 2006, pp. 116–120.
- [16] T. J. Richardson, M. A. Shokrollahi, and R. L. Urbanke, "Design of capacity-approaching irregular low-density parity-check codes," *IEEE Transactions on Information Theory*, vol. 47, no. 2, pp. 619–637, Feb 2001.
- [17] J. Cardinal and G. V. Assche, "Construction of a shared secret key using continuous variables," in *Proceedings 2003 IEEE Information Theory Workshop (Cat. No.03EX674)*, March 2003, pp. 135–138.

- [18] S. Jayasooriya, M. Shirvanimoghaddam, L. Ong, G. Lechner, and S. J. Johnson, "A new density evolution approximation for LDPC and multi-edge type LDPC codes," *IEEE Transactions on Communications*, vol. 64, no. 10, pp. 4044–4056, Oct 2016.
- [19] H. Saeedi and A. H. Banihashemi, "On the design of LDPC code ensembles for BIAWGN channels," *IEEE Transactions on Communications*, vol. 58, no. 5, pp. 1376–1382, May 2010.
- [20] V. Rathi and R. Urbanke, "Density evolution, thresholds and the stability condition for non-binary LDPC codes," *IEE Proceedings - Communications*, vol. 152, no. 6, pp. 1069–1074, Dec 2005.
- [21] C. MEASSON, "Conservation laws for coding," Ph.D. dissertation, Citeseer, 2006.
- [22] D. Divsalar, S. Dolinar, C. R. Jones, and K. Andrews, "Capacity-approaching protograph codes," *IEEE Journal on Selected Areas in Communications*, vol. 27, no. 6, pp. 876–888, August 2009.
- [23] A. Shokrollahi and R. Storn, "Design of efficient erasure codes with differential evolution," in *2000 IEEE International Symposium on Information Theory (Cat. No.00CH37060)*, 2000, pp. 5–.
- [24] S.-Y. Chung, "On the construction of some capacity-approaching coding schemes," Ph.D. dissertation, Massachusetts Institute of Technology, 2000.
- [25] T. J. Richardson and R. L. Urbanke, "The capacity of low-density parity-check codes under message-passing decoding," *IEEE Transactions on Information Theory*, vol. 47, no. 2, pp. 599–618, Feb 2001.
- [26] S. Jayasooriya, S. J. Johnson, L. Ong, and R. Berretta, "Optimization of graph based codes for belief propagation decoding," in *2014 IEEE Information Theory Workshop (ITW 2014)*, Nov 2014, pp. 456–460.